

# A Generalized Reaction–Diffusion Model With Explicit H–H<sub>2</sub> Dynamics for Negative-Bias Temperature-Instability (NBTI) Degradation

Haldun Küflüoğlu, *Student Member, IEEE*, and Muhammad Ashraful Alam, *Fellow, IEEE*

**Abstract**—In this paper, negative-bias temperature-instability (NBTI) modeling, based on a generalized reaction–diffusion framework, is presented. Unlike the previous models, the release of atomic hydrogen from the Si–H bonds at the Si/oxide interface and its subsequent conversion into molecular H<sub>2</sub> are considered without the (unphysical) assumption of instantaneous transition. The conversion reactions are handled explicitly with finite transition time, and numerical solutions that contain both H and H<sub>2</sub> dynamics are obtained. The conversion reactions result in a distinct time behavior which cannot be predicted from either H- or H<sub>2</sub>-only simulations. The results are then explained analytically. The implications of hydrogen conversion dynamics on saturation of NBTI characteristics and device lifetimes are also discussed.

**Index Terms**—Hydrogen, MOSFET, negative-bias temperature-instability (NBTI), reliability, saturation, time-dependence.

## I. INTRODUCTION

NEGATIVE-BIAS temperature-instability (NBTI) is a significant reliability concern for digital and analog circuits in current generation CMOS technology [1], [2]. NBTI occurs in negatively biased ( $V_{GS} < 0$  V) PMOSFETs at elevated temperatures and is a consequence of interface-trap generation at the Si/oxide interface. In conventional Si MOSFETs, the transistors are annealed in hydrogen ambient to passivate the dangling Si bonds during manufacture. This traditional method proved to be an effective solution to the interface-trap instabilities for decades; however, the continuing MOSFET miniaturization trends (i.e., aggressive oxide-thickness scaling leading to higher oxide field and process modifications, such as nitridation of oxides to prevent Boron diffusion from p+ poly gate) and higher operation temperatures (due to power dissipation from the circuits or ambient conditions) accelerate bond-breaking at the interface over time during the device operation. The traps shift the threshold voltage, reduce the channel mobility due to scattering, and induce parasitic capacitances in the transistors. Overall, the drain-current degrades over time, and parametric reliability becomes a significant concern.

The reaction–diffusion (R–D) framework has provided the theoretical understanding of NBTI phenomena. In this model, the characteristic power-law ( $t^n$ ) time-dependence of the

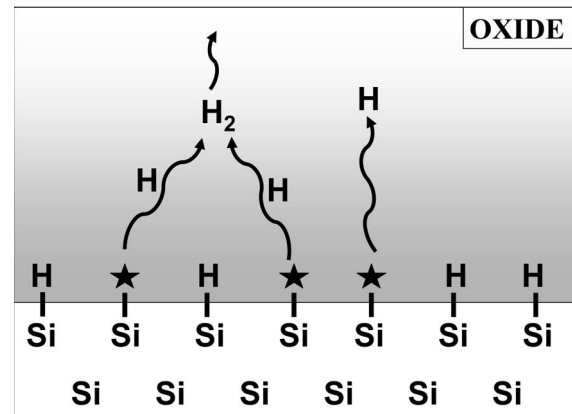


Fig. 1. Schematic of hydrogen dynamics after it is released from a Si–H bond. Interface traps are denoted by \*. Atomic hydrogen can diffuse away from the interface freely (traditional NBTI with exponent  $n = 1/4$ ) or forms H<sub>2</sub> with another H. Recent experiments suggest H<sub>2</sub> diffusion due to the activation energy of degradation.

degradation is attributed to the diffusion rate of hydrogen released from Si–H bonds at the Si/oxide interface [3]. Traditional R–D model has considered atomic H diffusion as the factor that shapes the time-exponent of NBTI. Recent measurements show that the activation energy of NBTI suggests H<sub>2</sub> diffusion with a time-exponent  $n$  of  $1/6$  [6], [7]. If the diffusing species is H<sub>2</sub>, atomic H released from the Si–H bonds during stress must be converted into H<sub>2</sub>, as illustrated in Fig. 1. Previous attempts that include H<sub>2</sub> diffusion in NBTI have not handled this conversion mechanism explicitly but rather assumed instantaneous transition [8], [9]. Therefore, as to whether noninstantaneous H ↔ H<sub>2</sub> transition modifies NBTI time-exponent is of interest. One of the major shortcomings of existing H<sub>2</sub> diffusion model for NBTI is that it is not obvious that once H ↔ H<sub>2</sub> transition is accounted for, the  $1/6$  exponent will remain robust. Our analysis completes the theoretical basis of the H ↔ H<sub>2</sub> model, interprets the origin of robust  $1/6$  exponent and the role of H as an interface layer.

In this paper, we present the theoretical background along with numerical solutions that incorporate the dynamics of hydrogen with a generalized approach that fills a fundamental technical gap in the R–D framework. In Section II, traditional R–D model for H-only diffusion is discussed and extended to H<sub>2</sub>-only diffusion. Then, the general scheme that contains both H and H<sub>2</sub> diffusion and the reactions between them is described. We present the analytical and numerical results in Section III, also explained the distinct early time behavior, and compared

Manuscript received September 21, 2006; revised January 8, 2007. This work was supported by the National Science Foundation (NSF)/Semiconductor Research Corporation (SRC) Joint Contract 2004-HJ-1238. The review of this paper was arranged by Editor G. Groeseneken.

The authors are with the School of Electrical and Computer Engineering, Purdue University, West Lafayette, IN 47906-1285 USA.

Digital Object Identifier 10.1109/TED.2007.893809

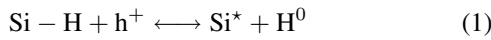
with experimental data presented in the literature. Finally, the conclusions are given in Section IV.

## II. NBTI THEORY

### A. Standard R-D Framework for H Diffusion

The modeling of NBTI through the R-D framework can successfully explain several experimental observations such as: 1) fractional time-exponents [11]; 2) activation energies [12]; 3) relaxation dynamics of degradation [13]; 4) frequency-dependence under ac stress [8], [13]; 5) isotope (i.e., deuterium) effects [14]; 6) lock-in mechanism [15]; and 7) quasi-saturation of NBTI [16].

In the R-D model, the interface-trap generation at the Si/oxide interface is represented as a chemical reaction, i.e.,



in which an inversion-layer hole  $\text{h}^+$  weakens a Si-H bond and hydrogen is detached as a result of thermal vibrations of the chemical bond [17]. The remaining Si dangling bond ( $\text{Si}^*$ ) acts as a donorlike interface trap [18]. The H released from the bond can diffuse away from the Si/oxide interface or anneal an existing trap. The interface-trap density  $N_{\text{IT}}$  increases with the net rate of the reaction given in (1), so

$$\frac{dN_{\text{IT}}}{dt} = k_F[N_0 - N_{\text{IT}}] - k_R N_{\text{IT}} N_{\text{H}}^{(0)} \quad (2)$$

where  $k_F$ ,  $k_R$ ,  $N_0$ , and  $N_{\text{H}}^{(0)}$  are bond-breaking, bond-annealing, Si-H bond density available before stress, and hydrogen density at the Si/oxide interface, respectively. When a device is stressed, initially, both  $N_{\text{IT}}$  and  $N_{\text{H}}^{(0)}$  are negligible ( $N_0 \gg N_{\text{IT}}$ ) and so is the  $k_R N_{\text{IT}} N_{\text{H}}^{(0)}$  term in (2). Therefore, the increase in  $N_{\text{IT}}$  is generation-limited. When sufficient hydrogen builds up at the interface, the diffusion of H away from the traps dominate, so the interface-trap generation rate becomes limited to the diffusion of hydrogen and, thus, represents the characteristic time evolution of NBTI degradation. In this period, the diffusion of hydrogen obeys

$$\frac{dN_{\text{H}}}{dt} = D_{\text{H}} \frac{d^2 N_{\text{H}}}{dy^2} \quad (3)$$

where  $D_{\text{H}}$  is the diffusion constant. From (2) and (3), it is obvious that the temperature and electric-field-dependence of NBTI is not considered explicitly in the R-D model. The oxide-field-dependence is included in the  $k_F$  term, and the temperature-dependence of the degradation is incorporated through the activation energies of  $k_F$ ,  $k_R$ , and  $D_{\text{H}}$  [19]. The rates  $k_F$  and  $k_R$  contain the microscopic details of the Si-H bond breaking and annealing of  $\text{Si}^*$  and reflect the associated activation energies as distributions over the energy range [20]. The effective bond-breaking and annealing rates can be written as

$$k_{F,R} = \int_0^{\infty} k_{F,R}^0 e^{\left(\frac{-E}{k_{\text{BT}}}\right)} \cdot g_{F,R}(E) dE \quad (4)$$

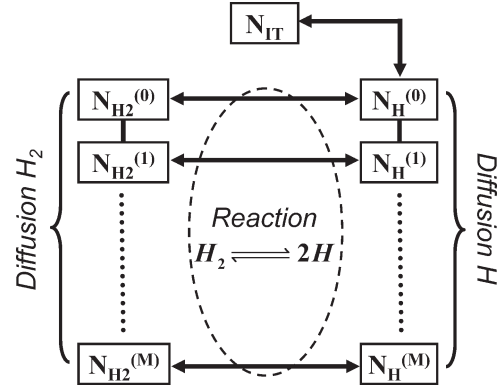


Fig. 2. Schematic representation of the numerical implementation for the generalized  $\text{H} \leftrightarrow \text{H}_2$  simulations. Both H and  $\text{H}_2$  dynamics are handled explicitly. The standard R-D model with H diffusion ignores  $\text{H}_2$  generation. The  $\text{H}_2$ -only model assumes instantaneous conversion; therefore, the H branch is not included. The simulation domain is discretized into  $M$  nodes, first node being the  $N_{\text{IT}}$  term. The rest of the nodes have H and  $\text{H}_2$  densities at the same physical location.

where  $g_{F,R}(E)$  is the Gaussian distribution [with mean  $E_A$  and variance  $(\Delta E_A)^2$ ] of the bond-activation energies.

The time-dependence of NBTI is governed by the slower process which is the diffusion in the R-D model. Therefore, any spread of activation energies in  $k_{F,R}$  has negligible effect on the time-dependence when superimposed on the diffusion mechanism [16].

When a Si-H breaks, every dangling Si bond is associated with a free H atom in the oxide; therefore,  $N_{\text{IT}}(t) = \int N_{\text{H}}(r, t) d^3r$ . The density of H in the oxide during diffusion can be approximated with a triangular profile, broadening as  $\sqrt{(D_{\text{H}} \cdot t)}$ . Then, the interface-trap density is given by

$$\begin{aligned} N_{\text{IT}}(t) &= \int_0^{\sqrt{D_{\text{H}}t}} N_{\text{H}}^{(0)} \left(1 - \frac{y}{\sqrt{D_{\text{H}}t}}\right) dy \\ &= \frac{N_{\text{H}}^{(0)}}{2} \sqrt{D_{\text{H}}t}. \end{aligned} \quad (5)$$

During the diffusion-dominated regime, the  $(dN_{\text{IT}})/(dt)$  term is negligible compared to the other bond-breaking and annealing terms in (2); therefore, (2) can be simplified as

$$N_{\text{IT}} N_{\text{H}}^{(0)} = \frac{k_F N_0}{k_R}. \quad (6)$$

Substituting  $N_{\text{H}}^{(0)}$  from (5) into (6), we obtain

$$N_{\text{IT}}(t) = \sqrt{\frac{k_F N_0}{2k_R}} (D_{\text{H}}t)^{\frac{1}{4}} \quad (7)$$

which gives the time-exponent ( $n = 0.25$ ) of NBTI when only H diffusion is taken into account. The derivations up to (7) correspond to H-diffusion branch in Fig. 2; therefore, the generation and diffusion of  $\text{H}_2$  are ignored completely.

### B. R-D Modeling With $\text{H}_2$ -only Diffusion

In the standard R-D model, only H diffusion is considered. However, it was shown that measurement-induced delays or

interruption of stress could yield time-exponents that are higher than the uninterrupted case [6], [7], [15]. Moreover, theoretical calculations suggest that atomic H is unstable and converted into molecular H<sub>2</sub> after it is released from the Si/oxide interface [17], [21]. Furthermore, activation energies extracted from NBTI measurements support that the dominant diffusing hydrogen species is H<sub>2</sub> [9], [10]. Therefore, a modified R-D modeling with H<sub>2</sub> can be obtained based on the principles of the H-only framework. In the H<sub>2</sub>-only model, after dissociation of Si-H bonds, released H atoms react and form the hydrogen molecule (see Fig. 1) as



Analytically, the derivations that yield (7) can be repeated when H<sub>2</sub> diffusion is the dominant factor that limits the degradation rate. The fundamental assumption in this modified model is that all atomic H becomes H<sub>2</sub> and only the H<sub>2</sub>-diffusion branch in Fig. 2 is taken into account. Once the H atoms react and generate H<sub>2</sub>, the change of the interface-trap density in (2) can be rewritten as

$$\frac{dN_{\text{IT}}}{dt} = k_F[N_0 - N_{\text{IT}}] - k_R N_{\text{IT}} N_{\text{H,eff}}^{(0)} \quad (9)$$

in which the annealing component has an effective hydrogen density term (and  $k_F$ ,  $k_R$  can be different from the H-only model). The  $N_{\text{H,eff}}$  is obtained by considering the equilibrium dynamics of (8), namely

$$N_{\text{H,eff}}^{(0)} \propto \sqrt{N_{\text{H}_2}^{(0)}}. \quad (10)$$

Additionally, corresponding to H<sub>2</sub> diffusion, (3) becomes

$$\frac{dN_{\text{H}_2}}{dt} = D_{\text{H}_2} \frac{d^2 N_{\text{H}_2}}{dy^2}. \quad (11)$$

The triangle approximation with H<sub>2</sub> diffusion away from the interface results in

$$N_{\text{IT}} = 2 \cdot \frac{1}{2} N_{\text{H}_2}^{(0)} \sqrt{D_{\text{H}_2} t} = N_{\text{H}_2}^{(0)} \sqrt{D_{\text{H}_2} t}. \quad (12)$$

The factor 2 in (12) comes from the fact that H<sub>2</sub> contains two H atoms, and therefore, it is associated with two interface traps. At the Si/oxide interface, (6) is still valid, and inserting (12) into (10) yields

$$N_{\text{IT}}(t) \propto \left[ \frac{k_F N_0}{k_R} \right]^{\frac{2}{3}} \cdot (D_{\text{H}_2} t)^{\frac{1}{6}}. \quad (13)$$

The H<sub>2</sub> diffusion and the time-exponent in (13) is consistent with the experimental activation energy of NBTI and time-dependencies observed in measurements.

### C. Generalized R-D Model With Both H and H<sub>2</sub> Diffusion

The H<sub>2</sub>-only R-D model employs assumptions stating that H-to-H<sub>2</sub> conversion is extremely fast, and H is consumed totally to generate H<sub>2</sub>. However, these assumptions may not be realistic, in general, for such a conversion reaction and the validity of

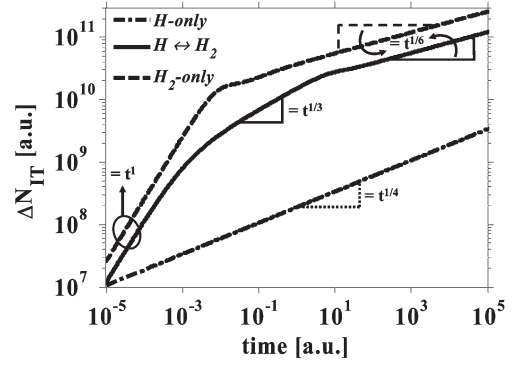


Fig. 3. When the conversion of H to H<sub>2</sub> is added into the simulations, the time-behavior changes significantly at earlier times. The diffusion mechanism in H-only and H<sub>2</sub>-only implementations cannot foresee this behavior. The H and H<sub>2</sub> results are the limiting cases for the H ↔ H<sub>2</sub> solution when the H<sub>2</sub> generation rate  $k_{\text{H}_1}$  is increased or decreased further.

the robust power-law time-dependencies predicted by H-only and H<sub>2</sub>-only models (also widely supported by experiments) is of concern. This issue can be addressed by a generalized modeling approach in which the aforementioned assumptions are relaxed by considering the dynamics of (8). In this approach, both H and H<sub>2</sub> branches in Fig. 2 are included, and their diffusion and mutual conversion are explicitly accounted for. According to (8), the rate of change in  $N_{\text{H}_2}$  is given by

$$\frac{dN_{\text{H}_2}}{dt} = k_{\text{H}_1} N_{\text{H}}^2 - k_{\text{H}_2} N_{\text{H}_2} \quad (14)$$

where  $k_{\text{H}_1}$  and  $k_{\text{H}_2}$  are generation and dissociation rates for H<sub>2</sub>. The rate for H can be written similarly. After Si-H bonds break, the released H atoms can diffuse away from the interface or get converted into H<sub>2</sub>. Although neutral H atom is thought to be unstable compared to the charged H ions in the oxide [22], in this model, the assumption is that the conversion into H<sub>2</sub> takes place very quickly, so neutral H<sup>0</sup> is possible under nonequilibrium conditions. The molecular H<sub>2</sub> can also diffuse or dissociates back to H atoms. Note that H<sub>2</sub> cannot be formed directly from the Si-H breaking nor it can passivate an interface trap. The complex nature of the dynamics in the generalized approach does not permit understanding the time-dependence of NBTI readily. Therefore, numerical solutions are needed to assess the effects of H-H<sub>2</sub> dynamics on NBTI degradation. The solutions are based on (2), (3), (11), and (14) and do not contain any approximations regarding the shape of the hydrogen profiles or restrict H-H<sub>2</sub> conversion reactions with specific assumptions. The details of the numerical implementation are presented in the Appendix.

## III. SIMULATION RESULTS AND DISCUSSION

The result of H ↔ H<sub>2</sub> simulation is compared with those of H-only and H<sub>2</sub>-only R-D numerical solutions in Fig. 3. As predicted by (7) and (13), H-only and H<sub>2</sub>-only simulations reflect the time-exponents of 1/4 and 1/6, respectively. The H-only and H<sub>2</sub>-only curves act as limits to the H ↔ H<sub>2</sub> result, i.e., as  $k_{\text{H}_1}$  in (14) reduces toward zero and H ↔ H<sub>2</sub> solution approaches that of H-only. Similarly, as  $k_{\text{H}_1}$  is increased further so that more H is consumed, the H ↔ H<sub>2</sub> result approximates

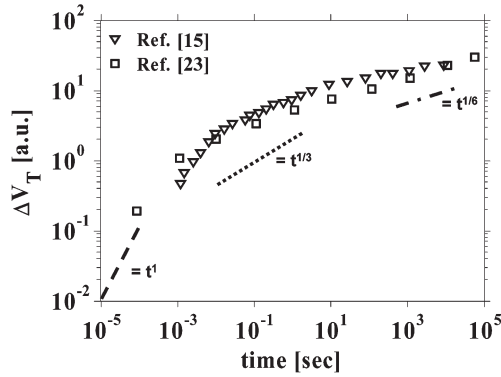


Fig. 4. Experimental data published in the literature shows a higher time-slope initially.  $H \leftrightarrow H_2$  theory supports the observations. Data from [15] and [23]. Note that  $\Delta V_T$  and  $\Delta I_{D,lin}$  are assumed to be proportional [2]. The  $\Delta V_T$  can include both interface charges and mobility degradation; however, at  $V_G \gg V_T$ , the mobility component is smaller due to the screening of inversion-layer holes.

the  $H_2$ -only solution. In Fig. 3, despite the fact that it gives the same result as  $H_2$ -only implementation at later times, the  $H \leftrightarrow H_2$  simulation shows a distinct behavior at earlier times. While the  $H_2$ -only model shows a sharp transition from  $t^1$  (reaction-dominated) to  $t^{1/6}$  (diffusion-dominated), the  $H \leftrightarrow H_2$  shows an intermediate soft-transition region with slope  $1 < n < 1/6$  ( $n \sim 1/3$  as in Fig. 3).<sup>1</sup> It is possible to use the interpretation of the exponent and prediction of early transition region (e.g.,  $< 10$  s) as a test for  $H \leftrightarrow H_2$  model. The time-exponent ( $1 < n < 1/6$ ) predicted by the theory supports experimental data presented in Fig. 4 [15], [23]. This change in the time-exponent is observed for a wide range of values of the  $k_{H_1}$  and  $k_{H_2}$  parameters, and the transition point where the exponent becomes  $1/6$  always denotes the beginning of the diffusion-dominated regime. The time-exponent of  $\sim 1/3$  in the  $H \leftrightarrow H_2$  solution can be explained by the aid of Figs. 5 and 6. In this regime, the atomic hydrogen released from the interface is being converted to  $H_2$  ( $dN_{H_2}/dt < 0$ ) according to (14), and thus,  $N_H^{(0)}$  keeps decreasing as  $N_{H_2}^{(0)}$  increases over time (see Fig. 5). Unlike (12), the diffusion in this regime is negligible, and since  $N_H^{(0)} \ll N_{H_2}^{(0)}$  due to the conversion,  $N_{IT} \propto N_{H_2}^{(0)}$  as verified by Fig. 6. Therefore,  $(dN_{IT}/dt) \propto (dN_{H_2}^{(0)}/dt)$  can be obtained. Also, from Fig. 6, although  $N_H^{(0)} \ll N_{H_2}^{(0)}$  at the Si/oxide interface, due to  $H_2$  generation,  $k_{H_1} [N_H^{(0)}]^2 \gg k_{H_2} N_{H_2}^{(0)}$  in (14). Substituting  $N_H^{(0)}$  from (6) gives

$$\frac{dN_{IT}}{dt} \propto \frac{dN_{H_2}^{(0)}}{dt} \propto k_{H_1} [N_H^{(0)}]^2 \propto \frac{1}{(N_{IT})^2}. \quad (15)$$

<sup>1</sup>At this point, it is important to recognize that a slightly different version of H-H<sub>2</sub> R-D model has been considered in the study in [7] and [8]: It considers H-H<sub>2</sub> conversion at the SiO<sub>2</sub>/poly interface rather than at the Si/SiO<sub>2</sub> interface, as presumed in this paper. Both models predict long-term  $n \sim 1/6$  regime and anticipate this transition regime ( $1 < n < 1/6$ ); however, the prediction is explicit and quantitative in our formulation (see Fig. 3) but implicit in the study in [7] and [8]. Since modern oxides are thin, any differences in the transition rates predicted by these models would be practically indistinguishable. In any case, the generalized framework presented in this paper can be easily modified to incorporate reaction at the SiO<sub>2</sub>/poly interface, if necessary and appropriate.

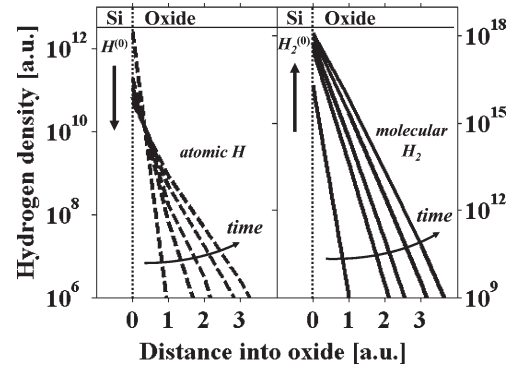


Fig. 5. Profiles of H (left panel) and  $H_2$  (right panel) during the  $N_{IT} \propto t^{1/3}$  regime. This period is marked by a significant consumption of H and its conversion into  $H_2$ . The  $H_2$  density is much higher than that of H. The diffusion is negligible so the profile tips extend only slightly with time and the change in densities of H and  $H_2$  at the interface is much more pronounced. Therefore,  $N_{IT} \propto N_{H_2}^{(0)}$ .

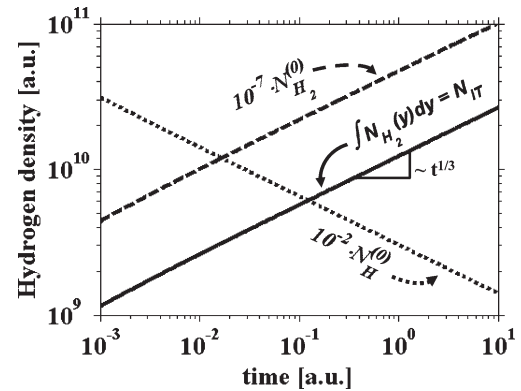


Fig. 6. During the  $N_{IT} \propto t^{1/3}$  regime, simulations show that the density of  $H^{(0)}$  decreases due to conversion into  $H_2$ .  $N_{H_2} \gg N_H$ , and since integrated,  $N_{H_2}$  and  $N_{H_2}^{(0)}$  are directly proportional,  $N_{IT} \propto N_{H_2}^{(0)}$ .

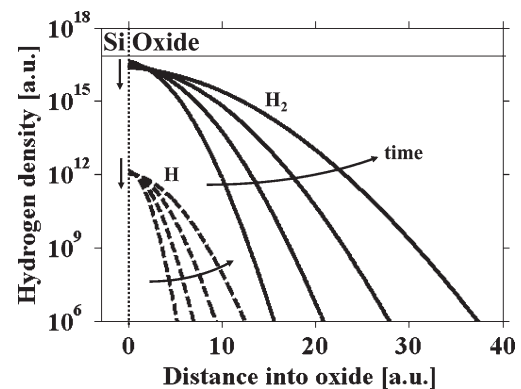


Fig. 7. After sufficient  $H_2$  buildup at the interface, diffusion begins to take over. The densities of H and  $H_2$  at the Si/oxide interface decrease with time, whereas the profile tips move as  $\sqrt{D_{hydrogen} \cdot t}$  (much faster compared to the profiles in Fig. 5), in accordance with the diffusion process. Both H and  $H_2$  diffuse but the density of H is much less than that of  $H_2$ , and the overall time-dependence of  $N_{IT}$  is limited by  $H_2$  diffusion  $n = 1/6$  regime.

The analytical solution of (15) gives  $N_{IT} \propto t^{1/3}$ , as observed in the numerical simulation results.

As the  $H_2$  density increases at the interface, eventually, it begins to diffuse away. As shown in Fig. 7, H also diffuses;

however, its density is much smaller than H<sub>2</sub>, so the interface-trap generation rate is governed by H<sub>2</sub> diffusion. Therefore, this behavior shifts the time-exponent to 1/6 at later times, in agreement with the analytical solution of (13).

The H ↔ H<sub>2</sub> model shows a transition behavior as the time-exponent changes from a higher value to 1/6 at earlier times. Note that this early time (< 10 s) transition is very different from the long-time (> 1000 s) quasi-saturation behavior observed in NBTI experiments. The quasi-saturation has been variously attributed to 1) reflection of diffusing species from material boundaries [8], 2) consumption of all Si-H bonds [16], [24], 3) distribution of bond energies [25], 4) experimental artifact arising from measurement delay (e.g., charge-pumping technique) [6], [26], 5) dispersive transport of H<sup>+</sup> species [27], etc.

These effects have been discussed in detail in [16]. It is now generally believed that long-term quasi-saturation is an artifact of measurement delay [6], [7], [16], [28] and would disappear once the measurement delays are accounted for. However, the short term (< 10 s) transient that we are discussing here is due to H-H<sub>2</sub> dynamics: This is a robust physical phenomenon and, in the absence of significant hole-trapping, should be visible even in no-delay measurements like on-the-fly measurements or ultrafast measurements.

This paper specifically deals with the R-D model, in which the degradation is attributed to interface-trap generation after Si-H breaking. Recent reports suggest that hole trapping/detrapping can also contribute to the overall NBTI degradation [23], [29], [30]. Since both N<sub>IT</sub> and hole trapping can affect NBTI, the time-dependence can depend on several factors: oxide-growth conditions (plasma/thermal nitridation), nitrogen concentration in the dielectric, oxide thickness, the measurement technique employed, possible measurement delay in characterization, the first time point and its subsequent use in degradation calculation, etc. [31], [32]. These factors are often not specified thoroughly in the reports, in turn, the process of distinguishing interface-trap and hole components becomes difficult. However, a recent systematic work points out that for technologically relevant thin oxides, the interface traps are mainly responsible for NBTI [32]. With the generalized R-D framework presented in this paper, the interface-trap contribution can be quantified from ΔV<sub>T</sub> or ΔI<sub>D,lin</sub> and any residual impact of hole trapping can be readily assessed.

#### IV. CONCLUSION

In this paper, we considered a generalized R-D model for H-to-H<sub>2</sub> conversion with finite-transition time. The time-behavior of NBTI is investigated when the dominant diffusing species is H<sub>2</sub>, and unlike previous attempts, the conversion of atomic H into H<sub>2</sub> is implemented explicitly in the numerical solutions. It is shown that the conversion of H to H<sub>2</sub> results in time-slopes higher than traditional NBTI time-slopes at earlier stress times. This time-dependence cannot be predicted from diffusion-only implementations.

The distinct time-dependence of the early part (< 10 s) degradation then can be used to assess the dominant hydrogen-

related mechanisms (H<sub>2</sub>-only or H-H<sub>2</sub>), the role of hole-trapping, or correct the artifacts due to first measurement point.

The experimentally observed soft-transition in the time-exponent in NBTI may stem from such conversion-dominated hydrogen dynamics.

If the measurement window is not long enough to allow the (soft) transition from  $n = 1$  to asymptotic  $n \sim 1/6$  region, the average NBTI time-exponent would be too large and the NBTI lifetime prediction by the data would be unnecessarily pessimistic. As such, one needs to exclude the initial soft-transition region before making lifetime predictions for NBTI degradation.

#### APPENDIX I NUMERICAL IMPLEMENTATION

To understand the implications of H-H<sub>2</sub> dynamics on NBTI degradation, the numerical model that incorporates both hydrogen species, their mutual coupling, and the exchange with Si-H bonds at the interface is developed. The diagram in Fig. 2 illustrates how the device domain is discretized, and the simulations are implemented. At the interface, the N<sub>IT</sub> term is coupled only to the N<sub>H</sub><sup>(0)</sup> term according to (1). The atomic hydrogen, once free from the interface, can diffuse away or gets converted into H<sub>2</sub>, as in (8). Similarly, H<sub>2</sub> can also diffuse or dissociates into two Hs. Notice that H<sub>2</sub> cannot be generated directly from the Si-H breaking.

Time-dependent Newton-Raphson method is used to construct the Jacobian matrix, which is given schematically as

$$\begin{bmatrix} \begin{bmatrix} n_{H_2}^{(M)} & \cdots & \cdot \\ \vdots & \ddots & \vdots \\ \cdot & \cdots & n_{H_2}^{(0)} \\ c_{H_2}^{(M)} & \cdots & \cdot \\ \vdots & \ddots & \vdots \\ \cdot & \cdots & c_{H_2}^{(0)} \\ \cdots & \cdots & \cdots \end{bmatrix} & \begin{bmatrix} c_H^{(M)} & \cdots & \cdot \\ \vdots & \ddots & \vdots \\ \cdot & \cdots & c_H^{(0)} \\ n_H^{(M)} & \cdots & \cdot \\ \vdots & \ddots & \vdots \\ \cdot & \cdots & n_H^{(0)} \\ \cdots & \cdots & a_{G-A} \end{bmatrix} & \begin{bmatrix} \cdot \\ \vdots \\ \cdot \\ \vdots \\ \cdot \\ a_{BC} \\ (n_{IT}) \end{bmatrix} \end{bmatrix} \cdot$$

The molecular and atomic hydrogen blocks, which are represented as  $n_{H_2}$  and  $n_H$  terms in the matrix, constitute the diffusing species. The conversion reactions between the H<sub>2</sub> and H are shown by coupling blocks [ $c_{H_2}$  and  $c_H$  from (14)]. The trap generation and annealing reaction in (1) is inserted into the  $a_{G-A}$  term along with the interface-trap density ( $n_{IT}$ ) term. Finally, to conserve the hydrogen and trap densities in the simulation, a boundary condition is implemented through the term  $a_{BC}$ . The boundary condition is obtained from a rate at which hydrogen changes at the Si/oxide interface [33], [34]. Implementing box integration at the interface gives

$$\frac{\Delta}{2} \frac{dN_H}{dt} = J_{inward} - J_{away} \quad (16)$$

where Δ is the grid spacing of the discretization in the domain,  $J_{inward}$  is the flux of H toward the Si/oxide interface, and  $J_{away}$  is the flux in the opposite direction. The  $J_{inward}$  is simply the interface-trap generation term  $dN_{IT}/dt$  from breaking of Si-H bonds and generating atomic H. The  $J_{away}$  encapsulates the

diffusion of the hydrogen species, H and H<sub>2</sub>, and their mutual conversion terms from (14). Therefore, the overall boundary condition can be written as

$$\frac{\Delta}{2} \frac{dN_H}{dt} = \frac{dN_{IT}}{dt} + J_H + 2 \cdot J_{H_2} + k_{H_2} N_{H_2} - k_{H_1} N_H^2 \quad (17)$$

The  $J$  represents the flux of the diffusing hydrogen species, i.e.,

$$J_X = D_X \frac{dX}{dy} \quad (18)$$

and the flux of H<sub>2</sub> is multiplied by two in (17), since a molecule contains two H atoms.

## APPENDIX II SIMULATION PARAMETERS

Throughout the simulations, the following parameters were used:  $k_F = 10^{-4} \text{ s}^{-1}$ ;  $k_R = 8 \times 10^{-9} \text{ cm}^3/\text{s}$ ;  $k_{H_1} = 10^{-5} \text{ cm}^3/\text{s}$ ;  $k_{H_2} = 10^{-1} \text{ s}^{-1}$ ;  $D_{H_2} = 4.0 \times 10^{-17} \text{ cm}^2/\text{s}$ ;  $D_H = 2.8 \times 10^{-17} \text{ cm}^2/\text{s}$ ; and  $T = 125 \text{ }^\circ\text{C}$ . The time-dependencies (time-exponents) of the degradation are independent of the parameters used above; they will only modify the magnitude of the degradation or shift in time. Since we are not fitting any particular experimental data in this paper, these parameter values were taken to be estimates of corresponding physical mechanisms.

## ACKNOWLEDGMENT

The authors would like to thank the Network for Computational Nanotechnology (NCN) for the resources provided at Purdue University, and A. E. Islam and D. Varghese for carefully reviewing the manuscript.

## REFERENCES

- [1] V. Reddy *et al.*, "Impact of negative bias temperature instability on digital circuit reliability," in *Proc. IEEE IRPS*, 2002, pp. 248–254.
- [2] A. T. Krishnan, V. Reddy, S. Chakravarthi, J. Rodriguez, S. John, and S. Krishnan, "NBTI impact on transistor and circuit: Models, mechanisms and scaling effects [MOSFETs]," in *IEDM Tech. Dig.*, 2003, pp. 349–352.
- [3] H. Küflüoğlu and M. A. Alam, "A geometrical unification of the theories of NBTI and HCI time-exponents and its implications for ultra-scaled planar and surround-gate MOSFETs," in *IEDM Tech. Dig.*, 2004, p. 113.
- [4] S. Mahapatra, B. P. Kumar, T. R. Dalei, D. Saha, and M. A. Alam, "Mechanism of negative bias temperature instability in CMOS devices: Degradation, recovery and impact of nitrogen," in *IEDM Tech. Dig.*, 2004, pp. 105–108.
- [5] M. L. Reed and J. D. Plummer, "Chemistry of Si–SiO<sub>2</sub> interface trap annealing," *J. Appl. Phys.*, vol. 63, no. 12, pp. 5776–5793, Jun. 1988.
- [6] D. Varghese, D. Saha, S. Mahapatra, K. Ahmed, F. Nouri, and M. A. Alam, "On the dispersive versus Arrhenius temperature activation of NBTI time evolution," in *IEDM Tech. Dig.*, 2005, pp. 684–687.
- [7] A. Krishnan *et al.*, "Material dependence of Hydrogen diffusion: Implications for NBTI degradation," in *IEDM Tech. Dig.*, 2005, pp. 688–691.
- [8] S. Chakravarthi, A. Krishnan, V. Reddy, C. F. Machala, and S. Krishnan, "A comprehensive framework for predictive modeling of negative bias temperature instability," in *Proc. IEEE IRPS*, 2004, p. 273.
- [9] A. Krishnan, S. Chakravarthi, P. Nicollan, V. Reddy, and S. Krishnan, "Negative bias temperature instability mechanism: The role of molecular hydrogen," *Appl. Phys. Lett.*, vol. 88, pp. 153 518:1–153 518:3, 2006.
- [10] J. P. Campbell, P. M. Lenahan, A. T. Krishnan, and S. Krishnan, "NBTI: An atomic scale defect perspective," in *Proc. IEEE IRPS*, 2006, pp. 442–447.
- [11] A. K. O. Jeppson and C. M. Svensson, "Negative bias of MOS devices at high electric fields and degradation of MNOS devices," *J. Appl. Phys.*, vol. 48, no. 5, pp. 2004–2014, May 1977.
- [12] S. Mahapatra, P. B. Kumar, and M. A. Alam, "A new observation of enhanced bias temperature instability in thin gate oxide p-MOSFETs," in *IEDM Tech. Dig.*, 2003, p. 337.
- [13] M. A. Alam, "A critical examination of the mechanics of dynamic NBTI for PMOSFETs," in *IEDM Tech. Dig.*, 2003, p. 345.
- [14] N. Kimizuka, K. Yamaguchi, K. Imai, T. Iizuka, C. T. Liu, R. C. Keller, and T. Horiuchi, "NBTI enhancement by nitrogen incorporation into ultrathin gate oxide for 0.10  $\mu\text{m}$  gate CMOS generation," in *VLSI Symp. Tech. Dig.*, 2000, p. 92.
- [15] S. Rangan, N. Mielke, and E. C. C. Yeh, "Universal recovery behavior of negative bias temperature instability," in *IEDM Tech. Dig.*, 2003, p. 341.
- [16] M. A. Alam and H. Küflüoğlu, "On quasi-saturation of negative bias temperature degradation," in *Proc. 208th Meeting ECS*, Oct. 2005.
- [17] S. T. Pantelides, S. N. Rashkeev, R. Buczko, D. M. Fleetwood, and R. D. Schrimpf, "Reactions of hydrogen with Si–SiO<sub>2</sub> interfaces," *IEEE Trans. Nucl. Sci.*, vol. 47, no. 6, pp. 2262–2268, Dec. 2000.
- [18] D. K. Schroder and J. A. Babcock, "Negative bias temperature instability: Road to cross in deep submicron silicon semiconductor manufacturing," *J. Appl. Phys.*, vol. 94, no. 1, pp. 1–18, Jul. 2003.
- [19] M. A. Alam and S. Mahapatra, "A comprehensive model of PMOS NBTI degradation," *Microelectron. Reliab.*, vol. 45, no. 1, pp. 71–81, Jan. 2005.
- [20] A. Stesmans, "Dissociation kinetics of hydrogen-passivated Pb defects at the (111) Si/SiO<sub>2</sub> interface," *Phys. Rev. B, Condens. Matter*, vol. 61, no. 12, pp. 8393–8403, Mar. 2000.
- [21] L. Tsetseris and S. T. Pantelides, "Migration, incorporation, and passivation reactions of molecular hydrogen at the Si–SiO<sub>2</sub> interface," *Phys. Rev. B, Condens. Matter*, vol. 70, no. 24, pp. 245 320–245 325, Dec. 2004.
- [22] J. Godet and A. Pasquarello, "Ab initio study of charged states of H in amorphous SiO<sub>2</sub>," *Microelectron. Eng.*, vol. 80, no. 1, pp. 288–291, Jun. 2005.
- [23] H. Reisinger *et al.*, "Analysis of NBTI degradation and recovery behavior based on ultra-fast  $V_T$  measurements," in *Proc. IRPS*, 2006, pp. 448–453.
- [24] S. Zafar, B. H. Lee, J. Stathis, A. Callegari, and T. Ning, "A model for negative bias temperature instability (NBTI) in oxide and high- $\kappa$  pFETs," in *VLSI Symp. Tech. Dig.*, 2004, pp. 208–209.
- [25] O. Penzin, A. Haggag, W. McMahon, E. Lyumkis, and K. Hess, "MOSFET degradation kinetics and its simulation," *IEEE Trans. Electron Devices*, vol. 50, no. 6, pp. 1445–1450, Jun. 2003.
- [26] N. K. Jha and V. R. Rao, "A new oxide trap-assisted NBTI degradation model," *IEEE Electron Device Lett.*, vol. 26, no. 9, pp. 687–689, Sep. 2005.
- [27] M. Houssa, M. Aoulaiche, S. De Gendt, G. Groeseneken, M. M. Heyns, and A. Stesmans, "Reaction-dispersive proton transport model for negative bias temperature instabilities," *Appl. Phys. Lett.*, vol. 86, no. 9, pp. 093 506 1–093 506 3, Feb. 2005.
- [28] M. Ershov *et al.*, "Dynamic recovery of negative bias temperature instability in p-type metal-oxide-semiconductor field-effect transistors," *Appl. Phys. Lett.*, vol. 83, no. 8, pp. 1647–1649, 2003.
- [29] M. Denais *et al.*, "On-the-fly characterization of NBTI in ultra-thin gate oxide PMOSFETs," in *IEDM Tech. Dig.*, 2004, pp. 109–112.
- [30] V. Huard and M. Denais, "Hole trapping effect on methodology for dc and ac negative bias temperature instability measurements in PMOS transistors," in *Proc. IEEE IRPS*, 2004, pp. 40–45.
- [31] A. Islam *et al.*, "Gate leakage vs. NBTI for plasma nitrided oxides: Characterization, physical principles and optimization," in *IEDM Tech. Dig.*, 2006, p. 12.4.1.
- [32] S. Mahapatra *et al.*, "On the physical mechanism of NBTI in silicon oxynitride p-MOSFETs: Can differences in insulator processing conditions resolve the interface trap generation versus hole trapping controversy?" in *Proc. IRPS*, 2007, to be published.
- [33] H. Küflüoğlu and M. A. Alam, "A computational model of NBTI and hot carrier injection time-exponents for MOSFET reliability," *J. Comput. Electron.*, vol. 3, no. 3, pp. 165–169, 2004.
- [34] H. Küflüoğlu and M. A. Alam, "Theory of interface-trap-induced NBTI degradation for reduced cross section MOSFETs," *IEEE Trans. Electron Devices*, vol. 53, no. 5, pp. 1120–1130, May 2006.



**Haldun Küflüoğlu** (S'04) received the B.S. and M.S. degrees in electrical engineering from Purdue University, West Lafayette, IN, in 2001 and 2003, respectively. He is currently working toward the Ph.D. degree at the same university. His Ph.D. research involves measurements and theoretical modeling of MOSFET degradation mechanisms such as NBTI, HCI, and TDDB, and their implications on VLSI design. Previously, he obtained micro-fabrication and testing skills in a MEMS sensor project that was interfaced with live neurons for

biological applications.

In 2006, he held a summer internship at Intel Corporation, LTD FE Q&R, Hillsboro, OR, where he worked on experimental 65-nm NBTI reliability and modeling.



**Muhammad Ashrafal Alam** (F'97) was with Bell Laboratories, Lucent Technologies, Murray Hill, NJ, from 1995 to 2001, as a Member of Technical Staff in the Silicon Ultra Large-Scale Integration Research Department. From 2001 to 2003, he was a Distinguished Member of Technical Staff at Agere Systems, Murray Hill. Since 2004, he has been a Professor of electrical and computer engineering with Purdue University, West Lafayette, IN, where his research and teaching focus on physics, simulation, characterization, and technology of classical and novel semiconductor devices, including theory of oxide reliability, nanocomposite thin-film transistors, and nanobiosensors. He has published over 80 papers in international journals and has presented many invited and contributed talks at international conferences.

Dr. Alam was the recipient of the 2006 IEEE Kiyo Tomiyasu Award for contributions to device technology for communication systems.